Control-oriented model of dielectrophoresis and electrorotation
for arbitrarily shaped objects

Tomáš Michálek, Aude Bolopion, Zdeněk Hurák, *Senior Member, IEEE,* and Michaël Gauthier

Abstract—The most popular modeling approach for dielectrophoresis (DEP) is the *effective multipole* (EM) method. Yet nowadays, in an unrestricted source electric field, a general multipolar description of the potential caused by their charge distribution is only available for spherical objects. We present a method for computing such multipolar representation of arbitrarily shaped objects polarized by arbitrary electric fields. The method is based on numerical solutions of Laplace equation for the potential and the orthonormality of spherical harmonics. We show how the superposition principle holding for the potential can be utilized to construct a basis of solutions, from which the total potential can be composed in real time. It is then possible to calculate the DEP forces and torques for arbitrarily shaped objects under the influence of arbitary electric fields in fractions of a second, which is needed in model-based control applications. This contrasts with the Maxwell stress tensor-based numerical method. We validate the proposed method against reference numerical solutions and analyse the importance of the higher-order multipolar moments using a sample case of a Tetris-shaped micro-object placed inside a quadrupolar micro-electrode array and exposed to electrorotation. The implementation of the model in Matlab and Comsol are offered for free download.

Index Terms—dielectrophoresis, non-spherical objects, arbitrarily-shaped objects, control-oriented model, electrorotation

I. INTRODUCTION

ELECTROKINETIC effects, when exploited at micro-scale, constitute a fundamental principle of numerous non-contact micro-manipulation devices. They use the electric field to impart forces and torques either directly on the objects of interest or indirectly on the liquid medium surrounding them, which then induces a fluid flow carying the objects to the desired locations.

A widespread representative of the former is the *dielectrophoresis* (DEP). First described by Pohl [1], it is a physical phenomenon enabling actuation of electrically neutral objects. By placing them in an nonhomogenous external electric field, they polarize and the newly emerged charge distribution inside them interacts via Coulomb forces with the source field. Alternating electric fields are commonly used to eliminate the (unwanted) phenomena of *electrolysis* and *electrophoresis*

T. Michálek and Z. Hurák are with Faculty of Electrical Engineering, Department of Control Engineering, Czech Technical University in Prague, Karlovo namesti 13, 121 35, Prague, Czech republic. E-mail: tomas.michalek@fel.cvut.cz.

A. Bolopion and M. Gauthier are with FEMTO-ST Institute, AS2M department Univ. Bourgogne Franche-Comt, CNRS, 24 rue Savary, F-25000 Besanon, France. Email: aude.bolopion@femto-st.fr.

(interaction between the possible intrinsic charge in the object and the external field). Two major modes of dielectrophoresis are distinguished: *conventional DEP* (cDEP) and *traveling-wave DEP* (twDEP). The former arises from a spatially varying *magnitude* of the field while the latter is due to a spatially varying *phase* of the field. The closely related concepts of *electroorientation* and *electrorotation*, both causing a torque acting on the object, are usually treated separately in the literature. A shared name—*generalized DEP* (gDEP), coined in [2], can be used to jointly describe all the above mentioned polarization-related phenomena. The review of gDEP may be found, for example, in [3], where the authors consider not only the quasi-static but also arbitrary time-varying fields. The latter is denoted as the *transient gDEP* or the *polarization history* (or *crossing trajectory*) effect. Since the period of the AC electric field is usually much higher than the time scale related to the object's movement, the quasi-static theory is usually sufficient.

A mathematical model of gDEP enables us not only to perform various simulations and analyses helping us to understand the described physics, but it is also necessary when it comes to applying gDEP to a precise position and orientation control of the micro-objects. In such cases, apart from the model accuracy, also its computational time becomes important as it is detailed in [4], where a device for independent position control of several micro-spheres is described. Following this motivation, we aim at developing a fast computational scheme for gDEP force and torque applicable not only to spheres, but to objects of arbitrary shapes.

State of the art

There are two basic approaches for modeling DEP: *effective moments method* (EM) [5]–[8] and *Maxwell stress tensor method* (MST) [6], [9]–[11]. The former approximates the polarized object by electric multipoles (the higher the order of the multipole, the higher the accuracy of the approximation) and provides an analytical formulas for the force and torque computation. Its use is, however, limited to spherical objects. The latter is applicable to completely general shapes, but imposes huge time and memory requirements due to the underlying finite element (FEM) simulations. For control purposes, we need the speed of EM and the possibility to treat also non-spherical objects provided by MST. Partial solutions exist for ellipsoidal objects [12], [13], where analytical formulas for induced dipole usable in EM are known, and also for arbitrary cylindrically symmetrical objects [14], [15], where

it is shown how multipolar moments up to the 9th order can be obtained from numerical simulations and then used in EM. In both cases, the symmetry requirement stems from the fact that only the linear multipoles are used for the description of the polarized object when all the charges' locations are constrained to a single line. Another related strong limitation of both approaches is that they are valid only if the external electric field is rotationally symmeteric.

Contribution

We propose a method of computing the multipolar moments of the polarized objects utilizing the numerical solution of Laplace equation for potential and the orthogonality property of the spherical harmonics. No limitation regarding the shape of the object, inhomogenity or direction of the source electric field are considered. We furhter use this method to construct a hybrid (consisting of some precomputed parts as well as expressions evaluated in real-time) control-oriented model, which can be evaluated in fractions of a second compared to units of hours in the case of a MST simulation. It serves as a solid foundation for future design of control algorithms with the forseen goal of achieving simultaneous DEP based position and orientation control of arbitrarily shaped micro-objects in fluidic mediums.

II. MATERIALS AND METHODS

A. Summary of the effective multipole method

To compute the gDEP force and torque acting on any polarized object placed in an inhomogeneous external electric field, we can simply use the formulas derived by Jones and Washizu in [5]

$$\langle \mathbf{F} \rangle = \sum_{n=1}^{N} \left\langle \mathbf{F}^{(n)} \right\rangle \tag{1}$$

$$\langle \mathbf{T} \rangle = \sum_{n=1}^{N} \left\langle \mathbf{T}^{(n)} \right\rangle, \tag{2}$$

where N is the order of approximation and

$$\left\langle \mathbf{F}^{(n)} \right\rangle = \frac{1}{2} \mathrm{Re} \left[\frac{\tilde{\boldsymbol{p}}^{(n)} [\cdot]^n (\nabla)^n \tilde{\mathbf{E}}^*}{n!} \right] \tag{3}$$

$$\left\langle \mathbf{T}^{(n)} \right\rangle = \frac{1}{2} \mathrm{Re} \left[\frac{1}{(n-1)!} \left[\tilde{\boldsymbol{p}}^{(n)} [\cdot]^{n-1} (\nabla)^{n-1} \right] \times \tilde{\mathbf{E}}^* \right]. \tag{4}$$

These expressions represent the EM method mentioned in the introduction. $\mathbf{F}^{(n)}$, resp. $\mathbf{T}^{(n)}$ is the force, resp. torque contribution caused by a multipole of order n. Regarding the notation, $\langle \cdot \rangle$ denotes the time average, $\mathrm{Re}[\cdot]$ takes just the real part of the expression, $\tilde{(\cdot)}$ is used to represent a phasor, $(\cdot)^*$ denotes a complex conjugate, ∇ is the gradient operator and the dyadic operation $[\cdot]^n$ means n dot multiplications. The only quantities we need to know to compute the force and torque are multipolar moments of orders $n = 1 \dots N$ denoted by $\tilde{\boldsymbol{p}}^{(n)}$ and a phasor $\tilde{\mathbf{E}}$ (and its corresponding spatial derivatives) of the external electric field $\mathbf{E}(\mathbf{x}, t) = \mathrm{Re} \left[\tilde{\mathbf{E}}(\mathbf{x}) e^{i\omega t} \right]$ at the given location.

The multipolar moments represent the electric potential arising from the charge distribution inside the polarized object being a consequence of the induced charge displacement. From a sufficiently far distance, this potential field seems to be generated just by a single point charge with a magnitude given by an integral over the whole charge distribution. If the object was electrically neutral, all the posive and negative charge introduced by the polarization principle should mutually cancel out and the mentioned integral should be equal zero. However, as we approach closer to the charge structure, it will be possible to distinguish some positive and negative areas, and an electric dipole could be a good approximation of such charge distribution. Even closer, more asymmetries in potential would be apparent, and thus quadrupoles or even higher order multipoles will have to be used to describe the considered charge distribution (and its potential field) accurately enough.

Formally, this can be shown by taking an arbitrary charge distribution $\rho(\boldsymbol{r})$ locally confined to an interior of some sphere S of radius R located, without the loss of generality, at the origin of the coordinate system. Outside this sphere, there is no charge. This situation may, for example, represent the alone polarized micro-object. The potential $\Phi(\boldsymbol{r})$ being created by such charge distribution (by the polarized object) may then be written in the following form

$$\Phi(\boldsymbol{r}) = \frac{1}{4\pi\epsilon_0} \int_{S(R)} \frac{\rho(\boldsymbol{r})}{|\boldsymbol{r} - \boldsymbol{r}'|} d^3 r', \tag{5}$$

where ϵ_0 is the permittivity of a vacuum and $\boldsymbol{r}$ is the location of the test particle. By expanding the term $\frac{1}{|\boldsymbol{r} - \boldsymbol{r}'|}$ in (5) in a Taylor series about the origin, we get

$$\Phi(\boldsymbol{r}) = \frac{1}{4\pi\epsilon_0} \cdot$$
$$\left\{ \frac{\boldsymbol{p}^{(0)}}{r} + \frac{\boldsymbol{p}^{(1)} \cdot \boldsymbol{r}}{r^3} + \frac{1}{2} \sum_{i,j=1}^{3} \frac{r_i r_j}{r^5} p_{ij}^{(2)} + \cdots \right\}, \tag{6}$$

where $r = \|\boldsymbol{r}\|_2$, r_i is the ith element of vector $\boldsymbol{r}$, $\boldsymbol{p}^{(n)}$ are the so-called *Cartesian multipolar moments* and $\boldsymbol{p}_{ij}^{(2)}$'s are the individual elements of quadrupolar moment $\boldsymbol{p}^{(2)}$. Since the sum is infinite, all the higher order moments are omitted from the listing. Notice that, in agreement with our following discussion, the higher the order of multipole is the faster it decays with the distance r from the object's position. If the potential being described was complex and represented by a phasor $\tilde{\boldsymbol{\Phi}}(\boldsymbol{r})$, also the multipolar moments would be complex and denoted by phasors $\tilde{\boldsymbol{p}}^{(n)}$ as for example in Eq. (3) and Eq. (4) .

B. Overview of the proposed modeling scheme

The problem of using the EM method for arbitrarily shaped objects was that up to now there was not any way for fast computation of their multipolar moments. Here, we show, how to overcome this limitation by employing the two key procedures: numerical computation of the multipolar moments and construction of a solution basis enabling us to do all the time demanding numerical simulations in advance and make the rest of the model evaluatable in real time.
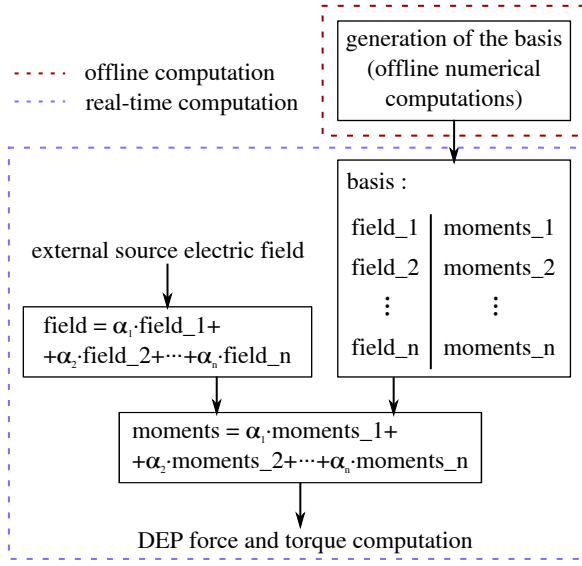
Fig. 1. Simplified diagram of the whole model.

In Fig. 1, there is s slightly oversimplified overview of the whole model highlighting its main working principles. We choose a set of orthogonal source electric fields (`field_1`, `field_2`, ..., `field_n`) and use them as a non-complete basis for an approximate description of the external electric field applied to the object of interest. We then use the coefficinets $\alpha_1, \alpha_2, \dots \alpha_n$ of the corresponding linear combination to compute the multipolar moments according to the diagram by using a basis table. This table is obtained in advance by a numerical method (described later on) and contains the multipolar moments of the object when polarized individually by fields `field_1`, `field_2`, ..., `field_n`. In the following sections, we will detail the individual blocks of the presented diagram.

C. Extraction of multipolar moments from numerical simulations

The multipolar moments are usually used in their Cartesian form as they appear for example in expressions Eq. (3) and Eq. (4) and throughout the previous subsection. In the following development we will, however, need to utilize some advantageous mathematical properties of the so-called spherical harmonics and therefore we will use a so-called *spherical form of multipolar moments* fitting better in the given framework.

These are obtained by performing the same expansion as in Eq. (6), but in spherical coordinates. Doing so, we get

$$\Phi(\boldsymbol{r}) = \frac{1}{4\pi\epsilon_0\epsilon_m} \sum_{l=0}^{\infty} \sum_{m=-l}^{l} \frac{4\pi q_{l,m}^*}{2l+1} \cdot \frac{Y_{l,m}(\theta,\phi)}{r^{l+1}}, \qquad (7)$$

where $q_{l,m}^* = \int r^l \rho(\boldsymbol{r},\theta,\phi) Y_{l,m}(\theta,\phi) dV$ are the components of the spherical form of multipolar moments. l is the order of the moment, and $m = -l \dots l$ denotes its elements. $Y_{l,m}(\theta,\phi) = \sqrt{\frac{(2l+1)(l-m)!}{4\pi(l+m)!}} P_{l,m}(\cos\theta) e^{im\phi}$ are the spherical harmonics defined using Legendre polynomials $P_{l,m}(\cos\theta)$.

$i = \sqrt{-1}$ denotes, as usual, the imaginary unit. Since $q_{l,m}$ is already a complex quantity, the extension of the above formula for complex potential $\tilde{\Phi}(\boldsymbol{r})$ is not so trivial as it was in the Cartesian case. Special care will have to be taken later on when complex potential will be needed.

Although the spherical form of multipolar moments varies from the Cartesian one, they both represent the same quantity. We can find expressions for mutual conversion between these two description by comparing the two expansions in Eq. (6) and Eq. (7) (as it is done for example in [16]). In the following text we will, for the reasons stated above, mostly utilize the spherical form and we will stress when the Cartesian one will be used.

For further development the property of orthonormality formally written as

$$\oint Y_{l,m}(\theta,\phi) Y_{l',m'}^*(\theta,\phi) d\Omega = \delta_{ll'}\delta_{mm'}, \qquad (8)$$

is of particular importance. In the expression above, δ_{ij} is the Kronecker delta and $d\Omega = \sin\theta d\theta d\phi$, since the integration is over a unit sphere. Other two useful properties are the following conjugation rules for spherical harmonics and spherical multipolar moments

$$q_{l,m}^* = (-1)^m q_{l,-m} \quad \text{and} \quad Y_{l,-m} = (-1)^m Y_{l,m}^*. \qquad (9)$$

Applying Eq. (8) and Eq. (9) to Eq. (7) enables us to express the multipolar moments.

At first, let's apply the first one to the potential expression in Eq. (7). We get

$$\Phi(\boldsymbol{r}) = \frac{1}{\epsilon_0\epsilon_m} \sum_{l=0,\infty} \sum_{m=-l,l} \frac{(-1)^m q_{l,-m}}{2l+1} \frac{Y_{l,m}(\theta,\phi)}{r^{l+1}}. \qquad (10)$$

Next, we change the order of summation and apply the second conjugation rule from Eq. (9). Then, we multiply both sides of the equation by $Y_{a,b}(\theta,\phi)$ and integrate them over a sphere $S(R)$. We obtain

$$\oint_{S(R)} \Phi(\boldsymbol{r}) Y_{a,b}(\theta,\phi) dS =$$
$$= \oint_{S(R)} \frac{1}{\epsilon_0\epsilon_m} \sum_{l=0}^{\infty} \sum_{m=-l}^{l} \frac{q_{l,m}}{2l+1} \frac{Y_{l,m}^*(\theta,\phi)}{r^{l+1}} Y_{a,b}(\theta,\phi) dS. \qquad (11)$$

Most of the terms on the right-hand side are independent on the integration variable and can be factored out in front of the integral. Thanks to the orthonormality of the spherical harmonics expressed in Eq. (8) and modified for a case of integration over a nonunit sphere to $\oint_{S(R)} Y_{a,b}^* Y_{a,b} dS = R^2$, the only summation term that remains is the one for $l = a$, $m = b$. This enables to express the multipolar moments as

$$q_{a,b} = \frac{(2a+1)\epsilon_0\epsilon_m}{R^{1-a}} \oint_{S(R)} \Phi(\boldsymbol{r}) Y_{a,b}(\theta,\phi) dS \qquad (12)$$

just based on the potential $\Phi(\boldsymbol{r})$ of the polarized object, which

voltages on electrodes

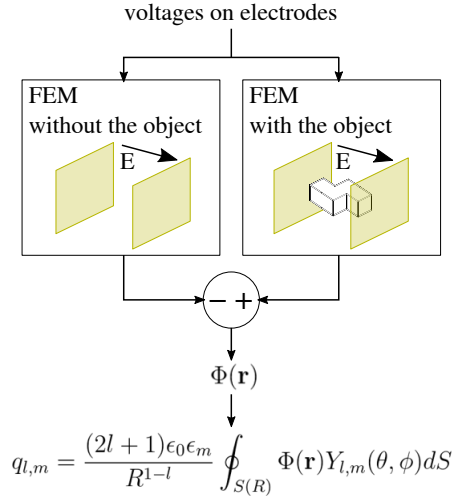$$q_{l,m} = \frac{(2l+1)\epsilon_0\epsilon_m}{R^{1-l}} \oint_{S(R)} \Phi(\mathbf{r}) Y_{l,m}(\theta,\phi) dS$$

Fig. 2. Illustration of the procedure for extracting the spherical multipolar moments $q_{a,b}$ of an arbitrary order for objects having an arbitrary shape.
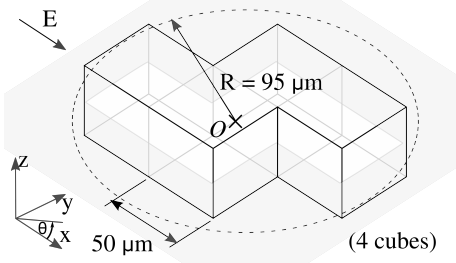

Fig. 3. Dimensions of the Tetris-shaped micro-object used in the example and validation simulations.
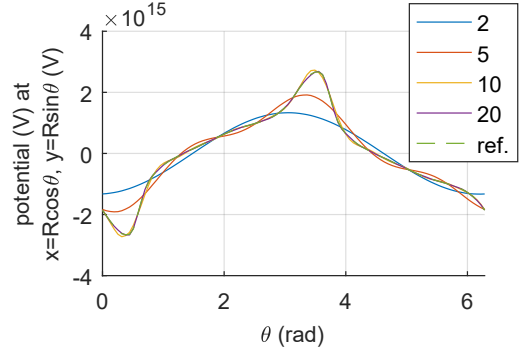

Fig. 4. Comparison of potentials along the circle laying in the xy-plane and enclosing the object as depicted in Fig. 3.

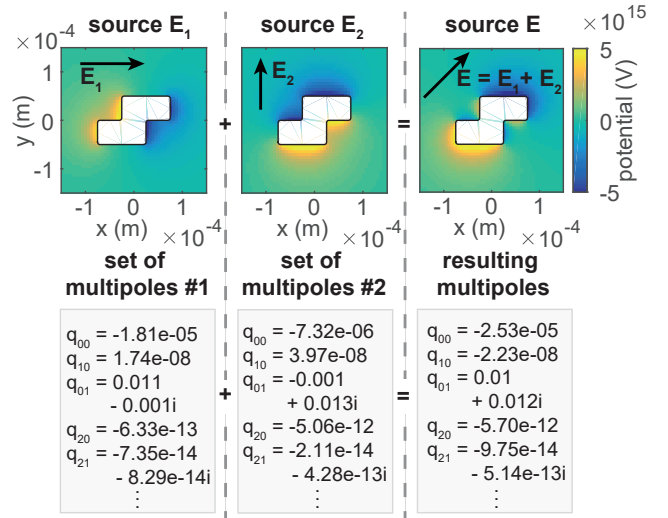Fig. 5. Illustration of the superposition principle utilization.

is easier to obtain than the unknown charge distribution that generates it. To get the potential, we simply numerically solve the corresponding Laplace equation for the two cases—one in a setting without the presence of the object of interest (just to get the source potential field) and the other including the object. By subtracting the source field from the second solution, we get the potential field $\Phi(\mathbf{r})$ corresponding to the polarized object itself. The whole procedure is illustrated in Fig. 2 for an example of a Tetris "S/Z"-shaped object placed in between two planar electrodes.

We use this example to demonstrate and prove the validity of the above described method. The object of interest is along-side with its dimensions in detail shown in Fig. 3. We used the method at first to compute its multipolar representation and then we plugged them into the Eq. (7) and compared the results against the solution obtained numerically using Comsol Multiphysics 5.1. External electric field with intensity of $1.1238 \cdot 10^{20}$ V/m pointing along the x-axis was used here. Fig. 4 showes the results for various orders of approximation.

In this section we have shown how a multipolar representation can be obtained for arbitrarily shaped and oriented objects located in arbitrary electric fields. After performing conversion from the spherical to Cartesian form, these multipolar moments could be used for DEP force and torque computation according to Eq. (3) and Eq. (4). Although this procedure may still be faster than using the Maxwell Stress Tensor

method, it does not eliminate the necessity for running a couple of numerical simulations every time the object changes its position or orientation, or when there is a change in the external electric field (for example the voltage signal applied to any of the electrodes changes). We will focus on this problem in the following section.

D. Construction of the solution basis

For the sake of simplicity, we will at first consider the orientation of the object to be fixed. In order to avoid repeated numerical computations, it is possible to utilize the principle of superposition holding for an electric potential (and as a consequence of Eq. (12) also for the multipolar moments). This means that knowing the multipolar descriptions of the object polarized by external fields $\mathbf{E}_1$, resp. $\mathbf{E}_2$, we can get the multipolar moments of the object polarized by $\alpha\mathbf{E}_1 + \beta\mathbf{E}_2$, $\alpha, \beta \in \mathbb{R}$ by the same linear combination of the corresponding known multipoles. See Fig. 5 for a simple illustrational example. It is depicted here how the multipolar moments for the field aligned along the diagonal direction can be obtained from the already known multipolar moments for the two separate cases of fields oriented along the horizontal and vertical directions.

TABLE I
VALUES OF qS USED IN COMPUTATION OF THE BASIS ELEMENTS

simulation #	$q_{0,0}^{\mathrm{S}}$	$q_{1,0}^{\mathrm{S}}$	$q_{1,1}^{\mathrm{S}}$	$q_{2,0}^{\mathrm{S}}$	$q_{2,1}^{\mathrm{S}}$	$q_{2,2}^{\mathrm{S}}$	$\cdots$
1	0	1	0	0	0	0	$\cdots$
2	0	0	1	0	0	0	$\cdots$
3	0	0	i	0	0	0	$\cdots$
4	0	0	0	1	0	0	$\cdots$
5	0	0	0	0	1	0	$\cdots$
6	0	0	0	0	i	0	$\cdots$
7	0	0	0	0	0	1	$\cdots$
8	0	0	0	0	0	i	$\cdots$
$\vdots$	$\vdots$	$\vdots$	$\vdots$	$\vdots$	$\vdots$	$\vdots$	$\ddots$

The basic idea is therefore to run the above described computational scheme for a suitable, rich enough set of source external electric fields and use the obtained results to form a basis—a table containing couples of the *source electric field* and the corresponding *multipolar representation* of the objects polarization. This should then enable us to perfom all the subsequent computations in real time without the need of any further numerical computations just as it is shown in Fig. 5. The only remaining problem is that in order to compute the multipolar representation of the object polarized by an arbitrary electric field (not only uniform one), the basis would need to have an infinite number of elements. Since we anyway have to chose and use some finite order of approximation n in EM based force and torque computations, it gives no sense to consider source electric fields with nonzero spatial derivatives of an order higher than $n-1$ in the process of basis construction. That is because polarization caused by such electric field could not be anyway represented by the considered multipolar moments.

Instead of representing the source electric field by its value and the value of its various spatial derivatives in the point of interest a more compact, and from the viewpoint of the numerical solutions to be performed, also more natural way of representing the source electric field is through the boundary potential conditions that generate it. For the purpose of the basis creation, we encapsulate the object by a large enough sphere $S(R')$ (so that the boundary effects would be negligible) centered at its center of gravity (or some other point we choose to compute the DEP force in) and by setting the potential on its interior surface we establish the source electric field. To get an orthonormal basis, we once again utilize the spherical harmonics and their orthonormality property. We use the expression Eq. (7) evaluated on the spherical boundary of the domain. By setting the qs, according to Table I and evaluating the above described scheme, we generate a set of mutually orthogonal basis elements. Note that the monopole term $q_{0,0}$ is always equal to zero since we assume that the object is electrically neutral. Further note that there are no negative indices related to qs. The reason is to save both computational time and storage space, as these can be determined by the above stated conjugation rules (Eq. (9)). Since spherical multipolar moments are in general complex

quantities, we have to also take into account their imaginary parts as can be seen for example in the 3rd, 6th or 8th row of Table I. An exception here are the elements $q_{a,0}$, $a \in \mathbb{Z}$, where the imaginary part is always equal to zero (this can be seen again from the conjugation rules in Eq. (9)).

The potential, $\tilde{\mathbf{\Phi}}^S$, resulting from such boundary conditions can alone generally be also complex even though the boundary potential condition applied to the sphere surface is purely real. The shift in phase leading to complex values is caused by the complex permittivity of the polarized object. As a consequence, two sets of multipolar moments have to be extracted from every simulation—one based on the real part of the potential field of the polarized object and the other based on its imaginary part. In contrast to the Cartesian representation of the multipolar moments, we can not use here the phasor notation (since the spherical multipoles are already complex quantitites) and we have to keep the two mentioned parts separately during storage as well as during subsequent computations making the notation slightly complicated. To summarize, from each simulation we will obtain and store $2 \cdot (1 + 2 + \cdots + n) = n(n+1)$ complex values being the elements of our basis.

Considering all of the above, we will use for a basis description a notation $q_{a,b}^{\mathrm{B},cde,\mathrm{f}}$, which denotes the element b of the spherical multipolar moment of order a resulting from a source electric field caused by a potential on $S(R')$. This potential is given by Eq. (7) with $q_{l,m} = 1$ when $l = c$, $m = d$ and $e = \mathrm{r}$ or by $q_{l,m} = i$ when $l = c$, $m = d$ and $e = \mathrm{i}$ ($q_{l,m} = 0$ for $l \neq c$ or $m \neq d$) and based on whether $f = \mathrm{r}$ or $f = \mathrm{i}$, only its real or imaginary part is considered. For example $q_{2,1}^{\mathrm{B},10\mathrm{i},\mathrm{r}}$ is the second element of the second order spherical multipolar moment extracted from a simulation when the source potential on $S(R')$ was given by real part of Eq. (7) evaluated with $q_{1,0} = i$ and all other qs being equal to zero.

In this section, we showed how the principle of superposition enables us to construct in advance a basis based on which multipolar moments resulting from any external field can be then computed in real time.

E. Decomposition of the source electric field

Having the basis and some arbitrary source electric field, for which we want to know the multipolar description of the polarized object, we now need to get the coefficients of the linear combination of the basis elements. As it was already stated above, these coefficients are exactly the same as are used in the linear combination of the corresponding source electric fields (see Fig. 5).

The source electric field is typically generated by some set of micro-electrodes. Knowing the voltage signals applied to the electrodes, we can compute the electric field at the object's location. In some specific cases of electrode designs an analytical solution may be known (for example for the so-called inter-digitated electrode arrays [17], [18]) in others one has to settle for the numerical solution. We used a partially analytical method based on Green's functions [19], which allowed us to compute high enough (in our case up to the 5th order) spatial derivatives of the electric field. In contrast to [19], we used a

slightly different discretization scheme. Instead of using semi-infinite rectangles suitable for the electrode array presented there, we divided the electrode plane into small enough square bins enabling us to approximate arbitrary electrode shapes.

For the purpose of basis generation we represented the source electric fields by the spherical moments q^{S} determining the potential boundary conditions for electric field generation. Now, we need to represent an arbitrary source field in the same way. In other words, we need to find such values of moments, which after plugging into expression Eq. (7) and evaluating it on the sphere $S(R')$ would give us a boundary condition corresponding to the source field.

In order to simplify things a little bit, let's for now assume that the source electric field is just real (the extension to the general complex case will follow in the subsequent section), which is the case when all the harmonic voltage signals applied to the electrodes have exactly the same phase. The multipolar description can then be found by at first using the well-known analytical expressions known for the Cartesian multipolar moments of a sphere [5] (expression 22):

$$\boldsymbol{p}^{\mathrm{E},(n)} = \frac{-4\pi\epsilon_0\epsilon_{\mathrm{m}}R'^{(2n+1)}}{(2n-1)!!}\nabla^{(n-1)}\mathbf{E}, \qquad (13)$$

and then just converting it to its spherical form. We denote the result as $q_{a0}^{\mathrm{E}}, q_{a1}^{\mathrm{E}}, \ldots, q_{aa}^{\mathrm{E}}$. These are then the desired coefficients of the linear combination of our precomputed basis elements. The resulting moments describing the real, respectively the imaginary part of the potential caused by the polarized object are then given by

$$q_{a,b}^{lr} = \sum_{c=1}^{n}\sum_{d=0}^{c}\mathrm{Re}\left[q_{c,d}^{\mathrm{E}}\right]q_{a,b}^{\mathrm{B},cdl,r}, \text{ where } l \in \{r,i\}, \qquad (14)$$

$$q_{a,b}^{li} = \sum_{c=1}^{n}\sum_{d=0}^{c}\mathrm{Im}\left[q_{c,d}^{\mathrm{E}}\right]q_{a,b}^{\mathrm{B},cdl,i}, \text{ where } l \in \{r,i\}. \qquad (15)$$

These spherical moments are then converted back to their Cartesian form $q_{0,n}^{lm}, q_{1,n}^{lm}, \ldots q_{n,n}^{lm} \to \boldsymbol{p}^{(n),lm}$ where $l, m \in \{r,i\}$ and assembled the following way to just one complex Cartesian moment

$$\boldsymbol{p}^{(n)} = (\boldsymbol{p}^{(n),rr} + \boldsymbol{p}^{(n),ri}) + i(\boldsymbol{p}^{(n),ir} + \boldsymbol{p}^{(n),ii}). \qquad (16)$$

In this form they can be finally used to compute the dielectrophoretic force and torque.

F. Considering complex potentials

In a case when the source potential itself can be complex (e.g. when there are phase-shifted signals applied to the electrodes), we will have instead of just one set of linear combination coefficients $q_{a0}^{\mathrm{E}}, q_{a1}^{\mathrm{E}}, \ldots, q_{aa}^{\mathrm{E}}$, two such sets: $q_{a0}^{\mathrm{E,r}}, q_{a1}^{\mathrm{E,r}}, \ldots, q_{aa}^{\mathrm{E,r}}$ and $q_{a0}^{\mathrm{E,i}}, q_{a1}^{\mathrm{E,i}}, \ldots, q_{aa}^{\mathrm{E,i}}$ representing the real respectively the imaginary part of the external electric field. The linear combination of the basis elements is then simply extended to

$$q_{a,b}^{klr} = \sum_{c=1}^{n}\sum_{d=0}^{c}\mathrm{Re}\left[q_{c,d}^{\mathrm{E},k}\right]q_{a,b}^{\mathrm{B},cdl,r}, \text{ where } k,l \in \{r,i\}, \quad (17)$$
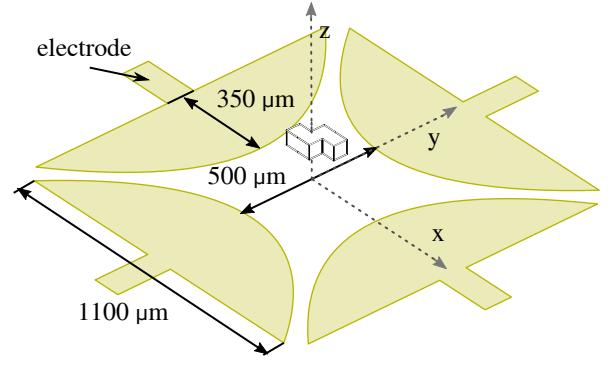

Fig. 6. Dimensions of the electrode array and Tetris-shaped micro-object used in the validation simulations.

$$q_{a,b}^{kli} = \sum_{c=1}^{n}\sum_{d=0}^{c}\mathrm{Im}\left[q_{c,d}^{\mathrm{E},k}\right]q_{a,b}^{\mathrm{B},cdl,i}, \text{ where } k,l \in \{r,i\}, \quad (18)$$

and the resulting spherical moments are then again converted to their Cartesian form and combined the following way

$$\boldsymbol{p}^{(n)} = \left((\boldsymbol{p}^{(n),rrr} + \boldsymbol{p}^{(n),rri}) + i(\boldsymbol{p}^{(n),rir} + \boldsymbol{p}^{(n),rii})\right) + \\ i\left((\boldsymbol{p}^{(n),irr} + \boldsymbol{p}^{(n),iri}) + i(\boldsymbol{p}^{(n),iir} + \boldsymbol{p}^{(n),iii})\right) \qquad (19)$$

to get the one resulting Cartesian moment suitable for DEP force and torque computations along Eq. (3) and Eq. (4).

G. Considering orientation of the object

So far, we have assumed that the orientation of the object is fixed. In practice, however, the manipulated object can revolve freely in the space and thus change its orientation. This slight complication can be simply solved by expressing the electric field and its necessary spatial derivatives in a new rotated frame of reference always attached to the object. After performing the force and torque computation, the results have to be again translated into the original global coordinate system. This can be accomplished by simply multiplying the resulting vectors by a corresponding rotational matrix.

III. RESULTS AND DISCUSSION

To prove the validity of the model, we compared its outcomes against the MST reference numerical simulations done in Comsol Multiphysics 5.1. A Tetris "S/Z" piece depicted in Fig. 3 was used as an example of an object, for which the real-time force and torque computations were so far unavailable. The dimensions of the object are included in the picture. As a test scenario for validation of the results, we used the so-called quadrupolar electrode array, which is usually used for torque generation in electrorotation experiments, but it can equally easily generate a DEP force. It is shown together with all the relevant dimensions in Fig. 6. As the driving signals we used four sinusoidal waveforms having amplitudes 10, 10, 50 and 50 V, respectively, and phase shifts 0°, 90°, 180° and 270°, respectively. The object's orientation was set such that from its initial orientation (as depicted in Fig. 6) it was rotated by 45° and 25° subsequently about

Fig. 7. Comparison of the force prediction obtained by the described model and the reference MST model.
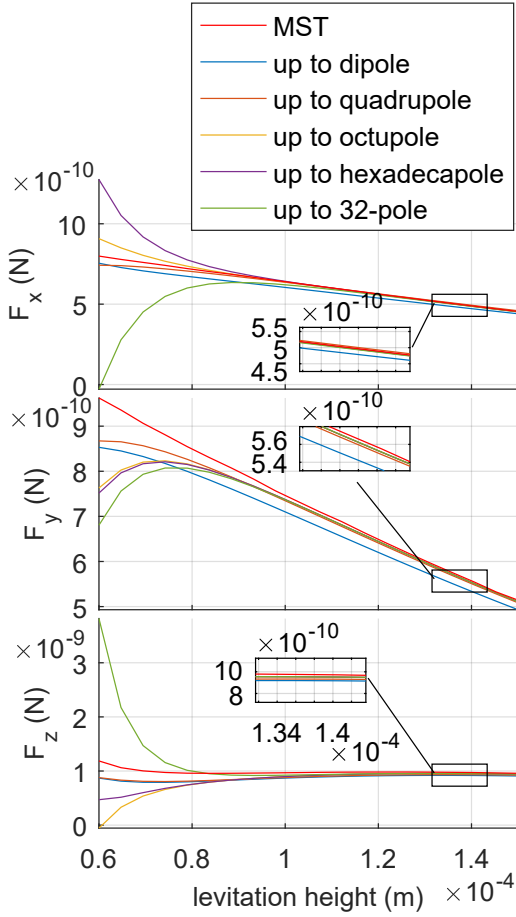

Fig. 8. Comparison of the torque prediction obtained by the described model and the reference MST model.

the x and y axes. Its geometric center was placed on the z axis. Several simulations for levitation heights varying between $60\,\mu\mathrm{m}$ and $150\,\mu\mathrm{m}$ were performed. To keep the errors negligible, we used moments up to the 5th order (32-poles). Note that to accurately represent polarization of non-spherical objects the higher order multipolar moments will be necessary even when the external electric field is uniform as could be already seen in the potential comparison shown in Fig. 4.

In Figures 7 and 8, we can see that results from our model resemble well the reference solution when high enough number of multipoles is used. As the object approaches the edges of the electrodes and the electric field around object becomes more inhomogeneous, the accuracy of the solution gets worse, since it would be necessary to use even more multipolar moments in such case to represent accurately the object's polarization.

During the simulations made above, we measured the times required for computation of DEP forces and torques by both the MST method and our proposed model. A conventional PC (Intel Core i5, $3.30\,\mathrm{GHz}$, 8 GB RAM, 64-bit, Win 7) was used. The results for different orders of approximation are stated in Table II. The evaluation of our model is clearly much faster than performing the numerical simulation for MST method. Nevertheless, with the increasing number of multipoles, the
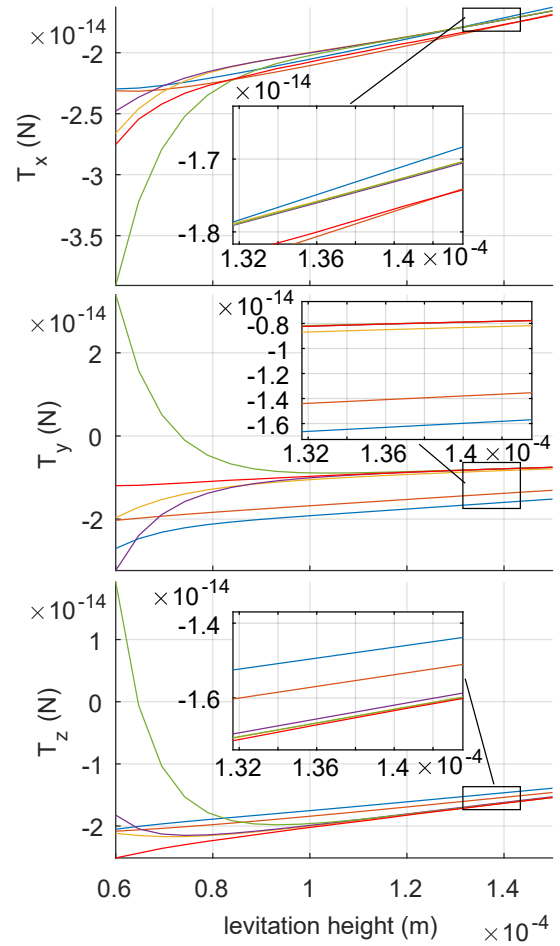
TABLE II
COMPARISON OF THE COMPUTATIONAL TIMES OF DIFFERENT MODELS

	Model	Computational time
EM method	$n = 1$ (dipole)	0.1 ms
	$n = 2$ (quadrupole)	0.2 ms
	$n = 3$ (octupole)	0.6 ms
	$n = 4$ (hexadecapole)	2.1 ms
	$n = 5$ (32-pole)	9.3 ms
	MST method	1 h 40 m 57 s

computational time t (in seconds) rises exponentially approximately according to $t = 9.768 \cdot 10^{-6} e^{1.37n}$, which means that the highest possible multipole computable under the time limit of $1\,\mathrm{s}$ would in the current implementation be the 256-pole ($n = 8$).

Since all the necessary numerical simulations can be done in advance (and just once for every new shape of the object), the real-time evaluation of the model takes only fractions of a second in comparison with hours of MST computation. Our Matlab implementation of the described mathematical model

can be found at [c1]www.example.com.

IV. CONCLUSION

We introduced a simulational scheme based on EM method capable of real-time computation of the DEP forces and torque acting on objects of arbitrary shapes under arbitrary orientations and located in arbitrary electric fields. The enabling ingredient is the usage of numerical solutions of the Laplace equation for getting the multipolar description of objects under such general scenarios. A specific way of how to construct a solution basis (from precomputed solutions) is then described so that all further computations can be done in real time. As such, the described control-oriented model could be used in future for simultaneous control of position and orientation of non-spherical objects with the envisioned biology and micro-assembly applications.

ACKNOWLEDGMENT

REFERENCES

[1] H. A. Pohl, *Dielectrophoresis: The Behavior of Neutral Matter in Nonuniform Electric Fields*. Cambridge ; New York: Cambridge University Press, Dec. 1978.

[2] X.-B. Wang, Y. Huang, F. F. Becker, and P. R. C. Gascoyne, "A unified theory of dielectrophoresis and travelling wave dielectrophoresis," *Journal of Physics D: Applied Physics*, vol. 27, no. 7, p. 1571, 1994. [Online]. Available: http://stacks.iop.org/0022-3727/27/i=7/a=036

[3] U. Lei and Y. J. Lo, "Review of the theory of generalised dielectrophoresis," *IET Nanobiotechnology*, vol. 5, no. 3, pp. 86–106, Sep. 2011. [Online]. Available: http://digital-library.theiet.org/content/journals/10.1049/iet-nbt.2011.0001

[4] J. Zemánek, T. Michálek, and Z. Hurák, "Feedback control for noise-aided parallel micromanipulation of several particles using dielectrophoresis," *Electrophoresis*, vol. 36, no. 13, pp. 1451–1458, Jul. 2015.

[5] T. B. Jones and M. Washizu, "Multipolar dielectrophoretic and electrorotation theory," *Journal of Electrostatics*, vol. 37, no. 1, pp. 121–134, May 1996. [Online]. Available: http://www.sciencedirect.com/science/article/pii/030438869600006X

[6] X. Wang, X.-B. Wang, and P. R. C. Gascoyne, "General expressions for dielectrophoretic force and electrorotational torque derived using the Maxwell stress tensor method," *Journal of Electrostatics*, vol. 39, no. 4, pp. 277–295, Aug. 1997. [Online]. Available: http://www.sciencedirect.com/science/article/pii/S0304388697001265

[7] T. B. Jones, "Basic theory of dielectrophoresis and electrorotation," *IEEE Engineering in Medicine and Biology Magazine*, vol. 22, no. 6, pp. 33–42, Nov. 2003.

[8] H. Morgan and N. G. Green, *AC Electrokinetic: Colloids and Nanoparticles*, 1st ed. Philadelphia, PA: Research Studies Pr, Jun. 2002.

[9] C. Rosales and K. M. Lim, "Numerical comparison between Maxwell stress method and equivalent multipole approach for calculation of the dielectrophoretic force in single-cell traps," *ELECTROPHORESIS*, vol. 26, no. 11, pp. 2057–2065, Jun. 2005. [Online]. Available: http://onlinelibrary.wiley.com/doi/10.1002/elps.200410298/abstract

[10] A. Benselama, P. Pham, and . Canot, *Modeling of the dielectrophoretic forces acting upon biological cells: A numerical comparison between Finite Element/Boundary Element Maxwell stress tensor methods and point-dipole approach*, Jan. 2018.

[11] T. Michálek and J. Zemánek, "Dipole and multipole models of dielectrophoresis for a non-negligible particle size: Simulations and experiments," *ELECTROPHORESIS*, vol. 38, no. 11, pp. 1419–1426, Jun. 2017. [Online]. Available: http://onlinelibrary.wiley.com/doi/10.1002/elps.201600466/abstract

[12] T. B. Jones, *Electromechanics of Particles*. Cambridge ; New York: Cambridge University Press, Sep. 2005.

[13] J. A. Stratton, *Electromagnetic Theory*. John Wiley & Sons, Jan. 2007, google-Books-ID: zFeWdS2luE4C.

[14] N. G. Green and T. B. Jones, "Numerical determination of the effective moments of non-spherical particles," *Journal of Physics D: Applied Physics*, vol. 40, no. 1, p. 78, 2007. [Online]. Available: http://stacks.iop.org/0022-3727/40/i=1/a=S12

[15] A. Ogbi, L. Nicolas, R. Perrussel, S. J. Salon, and D. Voyer, "Numerical Identification of Effective Multipole Moments of Polarizable Particles," *IEEE Transactions on Magnetics*, vol. 48, no. 2, pp. 675–678, Feb. 2012.

[16] S. Lea, "Spherical multipole moments," 2017. [Online]. Available: http://www.physics.sfsu.edu/ lea/courses/grad/sphermult.PDF

[17] T. Sun, H. Morgan, and N. G. Green, "Analytical solutions of ac electrokinetics in interdigitated electrode arrays: Electric field, dielectrophoretic and traveling-wave dielectrophoretic forces," *Physical Review E*, vol. 76, no. 4, p. 046610, Oct. 2007. [Online]. Available: http://link.aps.org/doi/10.1103/PhysRevE.76.046610

[18] D. E. Chang, S. Loire, and I. Mezi, "Closed-form solutions in the electrical field analysis for dielectrophoretic and travelling wave inter-digitated electrode arrays," *Journal of Physics D: Applied Physics*, vol. 36, no. 23, pp. 3073–3078, Dec. 2003. [Online]. Available: http://stacks.iop.org/0022-3727/36/i=23/a=032?key=crossref.d3a833ae1ca7f5df6d920ad280e82906

[19] M. Gurtner, K. Hengster-Movric, and Z. Hurk, "Green's function-based control-oriented modeling of electric field for dielectrophoresis," *arXiv:1703.01980 [physics]*, Mar. 2017, arXiv: 1703.01980. [Online]. Available: http://arxiv.org/abs/1703.01980

[c1]*TM*: fill in the proper web address

Michael Shell Biography text here.

PLACE
PHOTO
HERE

John Doe Biography text here.

Jane Doe Biography text here.